# Single-molecule junctions sensitive to binary solvent mixtures

Gregor Gurski [1], Henning Kirchberg [2], Peter Nalbach [3], and Michael Thorwart [1]

[1]*I. Institut für Theoretische Physik, Universität Hamburg, Notkestr. 9, 22607 Hamburg, Germany*
[2]*Department of Chemistry, University of Pennsylvania, Philadelphia, Pennsylvania 19104, USA*
[3]*Fachbereich Wirtschaft & Informationstechnik, Westfälische Hochschule, Münsterstr. 265, 46397 Bocholt, Germany*

We propose a quantum-mechanical model to calculate the nonlinear differential conductance of a single molecular junction immersed in a solvent, either in pure form or as a binary mixture with varying volume fraction. The solvent mixture is captured by a dielectric continuum model for which the resulting spectral density is determined within the Gladstone-Dale approach. The conductance of the molecular junction is calculated by a real-time diagrammatic technique. We find a strong variation of the conductance maximum for varying volume fraction of the solvent mixture. Importantly, the calculated molecular nonlinear conductance shows a very good agreement with experimentally measured data for common molecular junctions in various polar solvent mixtures.

## I. INTRODUCTION

The wiring of an individual molecule between two metallic leads has by now become a versatile technique for measuring its electronic transport characteristics as a basis for the miniaturization of electronic devices [1]. Aviram and Ratner first proposed the idea of utilizing single organic molecules as rectifiers [2]. Since then, there have been dramatic advances toward the realization of electronic transistors integrated on the molecular scale [3]. As a vital component of molecular electronics, single molecular junctions have attracted significant attention in both theory and experiment [1,4].

Not only was the first single-molecule transistor fabricated already in 2000 [5], but single-molecule junctions have been utilized as sensors [6] and have recently attracted much attention due to their promising thermoelectric properties [7,8]. The tuning of the energy level alignment of the molecule, e.g., the HOMO-LUMO gap, which is typically achieved via a gate electrode, plays a major role in single-molecule junctions. Thermoelectric properties, e.g., the Seebeck coefficient, can be readily enhanced when the dominant transport level is close to the chemical potential of the leads [9]. However, an additional gate electrode may lead to technical challenges for the integration because current leakage may occur [10]. To address this issue, solvent gating has been considered as a potentially simple method to continuously fine-tune the charge transport through single-molecule junctions. A strong influence of the surrounding solvent on the charge transport was recently reported for certain organic molecular junctions with different anchoring groups in various solvent environments using the break-junction technique [11]. The molecular conductance was shown to be tunable by nearly an order of magnitude by varying the polarity of solvent. Furthermore, gating efficiency due to solvent-molecule interactions was found to depend on the choice of the anchor group.

Theoretical description of the influence of the solvent has relied on utilizing density functional theory (DFT) calculations for the molecular orbitals. With this, the influence of pure polar solvents on molecular junctions has been predicted [12]. Yet a simple theoretical modeling on the basis of a few model parameters which provides understanding of the role of a solvent, or mixtures thereof, on charge transport is still lacking.

In this work, we propose a theoretical model of a molecular junction in a polar solvent described as a dielectric continuum. The latter forms a bosonic environment of fluctuating polarization modes which couple to a single excess electron in a molecular junction between two metallic electrodes. In particular, we consider pure solvents and miscible binary solvent mixtures. Using a quantum mechanical master equation, we calculate the junction's electric conductance in dependence on the fractional ratio of the solvent constituents and their respective chemical properties. We show that the influence of the polar solvent on the molecular conductance can be captured by its dielectric parameters. We compare the results of our theory to measured experimental data of the conductance of a molecular junction and find a very good agreement between calculated and experimentally determined data. The approach can readily be generalized to more complicated mixtures of solvents, giving rise to technical applications as concentration sensors on the molecular scale.

## II. MODEL

To study the charge current through the single molecular junction immersed in a polar solvent or a binary mixture thereof, we use the Hamiltonian

$$H = H_{\text{mol}} + H_{\text{leads}} + H_{\text{solv}} + H_{\text{mol}-\text{solv}} + H_{\text{tun}},$$

$$H_{\text{mol}} = \varepsilon_d d^\dagger d,$$

$$H_{\text{leads}} = \sum_{k,r=R,L} (\varepsilon_{k,r} - \mu_r) c_{k,r}^\dagger c_{k,r},$$

$$H_{\text{tun}} = \sum_{k,r=R,L} (t_{k,r} c_{k,r}^\dagger d + \text{H.c.}), \tag{1}$$
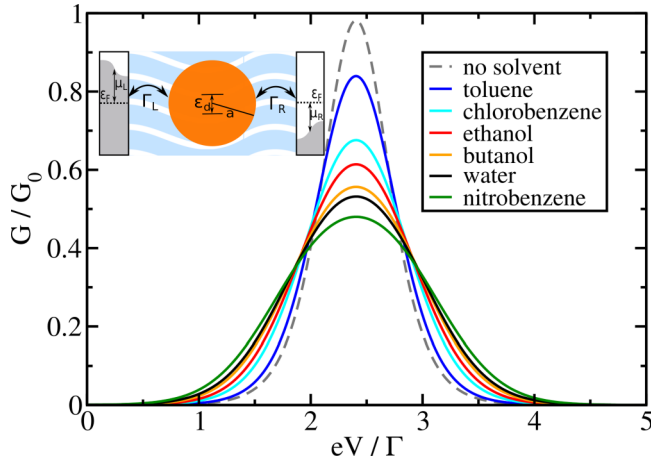
FIG. 1. Nonlinear differential conductance $G = dI/dV$ as a function of the bias voltage $V$ in the absence of a solvent (gray dashed line) and with various surrounding pure solvents (solid lines) as indicated. $G_0 = 2e^2/h$ is the conductance quantum. Parameters are $a = 5$ Å, $\Delta\mu = 5$ D, $T = 0.1\,\Gamma$, $\varepsilon_d = 1.2\,\Gamma$, and $\Gamma = 250$ meV. Inset: Sketch of the model of the molecular junction between two metallic leads and surrounded by a dielectric solvent.

with the annihilation operator $d$ for an electron on the molecule with energy $\varepsilon_d$, and with $c_{k,r}$ for an electron with energy $\varepsilon_{k,r}$ in the lead $r = L, R$ which is held at the chemical potential $\mu_r$, respectively (see inset of Fig. 1 for a sketch). We limit our consideration to two molecular electronic states, describing an oxidized state with $N$ and a reduced state with $N + 1$ electrons on the molecule. This standard assumption of strong Coulomb repulsion pushes states with other electronic occupations in energy regimes that are not accessible under the experimental conditions [11,13].

The tunneling hybridization between the molecular level and the corresponding lead $r$ is given by $\Gamma_r = 2\pi|t_{k,r}|^2 D(\varepsilon_F)$, where we assume as usual an energy-independent density of electronic states $D(\varepsilon_F)$ around the Fermi energy $\varepsilon_F \equiv 0$ within both leads (wide-band approximation). Throughout the work, the bias voltage $V$ is symmetrically applied around the Fermi energy, $\mu_L = -\mu_R = eV/2$, and the two tunneling barriers are assumed equal, i.e., $\Gamma_L = \Gamma_R = \Gamma$. Furthermore, we set $\hbar \equiv 1$ and $k_B \equiv 1$.

The polar solvent is described by its electric field modes with frequency $\omega_m$ created by the bosonic operator $a_m^\dagger$ (annihilated by $a_m$), which gives rise to the Hamiltonian [14,15]

$$H_{\text{solv}} = \sum_m \omega_m a_m^\dagger a_m. \tag{2}$$

The polarization modes couple to the electronic occupation of the molecule, with the interaction Hamiltonian

$$H_{\text{mol}-\text{solv}} = \sum_m g_m d^\dagger d(a_m^\dagger + a_m). \tag{3}$$

The parameter $g_m$ denotes the molecule-solvent coupling strength for each mode $m$ individually. Their collection is usually administered by the spectral density [14,15]

$$J(\omega) = \sum_m g_m^2 \delta(\omega - \omega_m). \tag{4}$$

In the following, we use a continuous Debye form of $J(\omega)$ which describes the dielectric properties of the solvent (mixture) within the Onsager model of quantum solvation. With this, the relevant solvent characteristics enter via its dielectric constants and the Debye relaxation time.

## III. SPECTRAL DENSITY FOR SOLVENT MIXTURES

We assume that the electronic charge distribution of the molecule is located inside a spherical Onsager cavity with radius $a$ (inset of Fig. 1), which reflects the size of the molecule, and with the vacuum dielectric constant of 1 [16]. Furthermore, the occupied and the empty molecular state are, for ease of the analysis, assumed to have dipole moments of different magnitude pointing in the same direction. We assume that the molecule adjusts its dipole moment when an excess electron enters or leaves the molecular junction due to changes of the overall molecular charge density. The resulting molecular dipole polarizes the solvent which induces a back-action (or reaction) electric field inside the cavity. This reaction field interacts with the dipole and mediates the leading coupling between the molecule and the solvent. Although this model, which is based on the Onsager model, does not include the microscopic details of the solvent, it captures the essential low-energy physics of the solvation process in the regime of long polarization wavelengths [14,15,17]. For instance, some organic molecules considered below in more detail, such as the standard oligophenylethynylene-sulfurmethyl (OPE-SMe)-bridge, possess dipole moments in the respective states [18–22].

The resulting spectral density incorporating the molecule-solvent interaction is found to be [17]

$$J(\omega) = \frac{(\Delta\mu)^2}{2\pi\varepsilon_0 a^3} \frac{6\varepsilon''(\omega)}{(2\varepsilon'(\omega) + 1)^2 + 4\varepsilon''(\omega)^2}, \tag{5}$$

where $\varepsilon_0$ is the vacuum permittivity, $a$ is the radius of the Onsager sphere, and $\Delta\mu$ is the change in magnitude of the dipole moment from the oxidized to the reduced state. Here $\varepsilon'(\omega)$ is the real and $\varepsilon''(\omega)$ is the imaginary part of the dielectric function of the solvent.

In order to describe binary mixtures we exploit the simplest approach of Gladstone and Dale for its effective dielectric function [23]

$$\varepsilon(\omega) = (1 - f)\varepsilon_h(\omega) + f\varepsilon_i(\omega), \tag{6}$$

which includes the relative concentrations of a host $(1 - f)$ and an inclusive $(f)$ solvent, with the dielectric permittivity $\varepsilon_h(\omega)$ and $\varepsilon_i(\omega)$, respectively. Inserting this effective dielectric function into Eq. (5), we obtain

$$J(\omega) = 2\eta_1 \frac{\omega\omega_1}{\omega^2 + \omega_1^2} + 2\eta_2 \frac{\omega\omega_2}{\omega^2 + \omega_2^2}, \tag{7}$$

where all parameters $\eta_1, \eta_2, \omega_1$, and $\omega_2$ depend on the relative volume fraction $f$, the high- and low-frequency dielectric constants of the host and of the inclusive solvent, and their respective Debye relaxation times (see Supplemental Material [24] for the detailed expressions). For $f \to 0$ (or $f \to 1$) the spectral density in Eq. (7) corresponds to that of the respective pure solvent, which has the Debye form [17] $J(\omega) = 2\eta\omega\omega_c/(\omega^2 + \omega_c^2)$. Here $\omega_c = \frac{2\varepsilon_S + 1}{2\varepsilon_\infty + 1}\tau_D^{-1}$ is the characteristic

**(a)** $J(\omega)/\eta_{\text{NBZ}}$

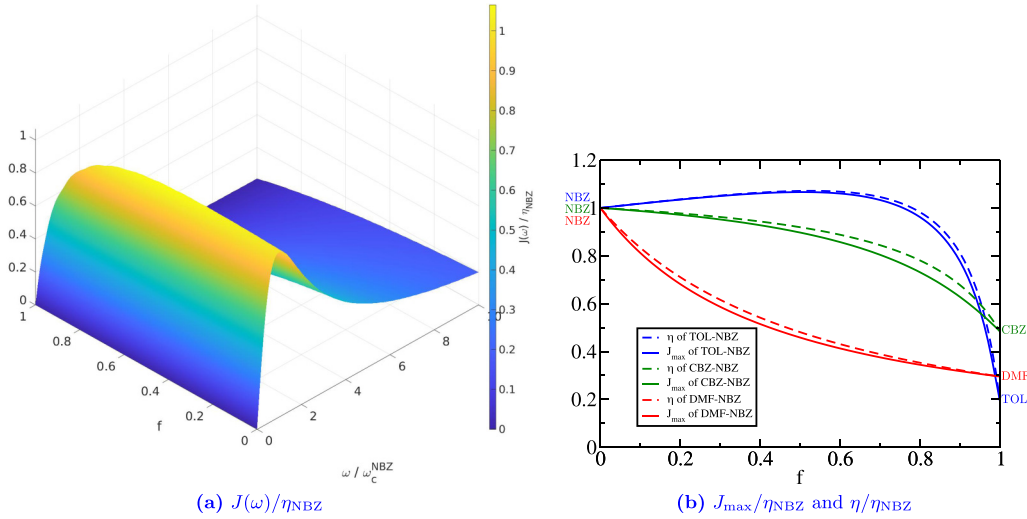**(b)** $J_{\max}/\eta_{\text{NBZ}}$ and $\eta/\eta_{\text{NBZ}}$

FIG. 2. (a) Spectral density $J(\omega)$ normalized to the reorganization energy $\eta_{\text{NBZ}}$ of nitrobenzene as a function of the volume fraction $f$ and the frequency $\omega$ (normalized to the cutoff frequency of nitrobenzene $\omega_c^{\text{NBZ}}$) for the solvent mixture between nitrobenzene and toluene. (b) Maximum of the spectral density as well as the reorganization energy $\eta$, both normalized to $\eta_{\text{NBZ}}$, for the solvent mixtures toluene-nitrobenzene, chlorobenzene-nitrobenzene, and dimethylformamide-nitrobenzene. The solvent parameters are given in Table S1 of the Supplemental Material [24].

cutoff frequency, where $\varepsilon_\infty$ and $\varepsilon_S$ are the high- and low- (static) frequency dielectric constants, respectively, and $\tau_D$ is the Debye relaxation time. The reorganization energy $\eta$ is related to the spectral density via [25]

$$\eta = \frac{1}{\pi}\int_0^\infty d\omega \frac{J(\omega)}{\omega} = \frac{(\Delta\mu)^2}{4\pi\varepsilon_0 a^3}\frac{6(\varepsilon_S - \varepsilon_\infty)}{(2\varepsilon_S + 1)(2\varepsilon_\infty + 1)}. \quad (8)$$

In Fig. 2(a) we show an exemplary plot of the spectral density for a solvent mixture between nitrobenzene and toluene. Additionally, in Fig. 2(b) we show the maximum of the spectral density $J_{\max}$ as well as the reorganization energy $\eta$ for the solvent mixtures toluene-nitrobenzene, chlorobenzene-nitrobenzene, and dimethylformamide-nitrobenzene. It can be observed that only for the mixture between nitrobenzene and toluene is $J_{\max}$ nonmonotonous, which subsequently results in the nonmonotonous behavior of the maximum differential conductance for this mixture; see Fig. 3 in the next section.

## IV. STATIONARY CURRENT AND CONDUCTANCE

The charge current in the lead $r = L, R$ is given by the time-dependent change of the number of elementary charges $e > 0$ as $\langle I_r(t)\rangle = e\frac{d}{dt}\langle N_r(t)\rangle = ie\langle[H_{\text{tun}}, N_r](t)\rangle$, where $N_r = \sum_k c_{rk}^\dagger c_{rk}$, which is equivalent to

$$\langle I_r(t)\rangle = -ie\sum_k (t_{k,r}\langle c_{k,r}^\dagger(t)d(t)\rangle - t_{k,r}^*\langle d^\dagger(t)c_{k,r}(t)\rangle), \quad (9)$$

where $\langle\cdots\rangle$ indicates the expectation value as the trace over all molecule, solvent, and lead degrees of freedom.

Using a quantum master equation according to Refs. [26–28], we obtain

$$\langle I_r(t)\rangle = -e\sum_{\psi_1'\psi_2'\psi_3}\int_{t_0}^t dt' P_{\psi_2'}^{\psi_1'}(t')\Sigma_{\psi_2'\psi_3}^{I_r\psi_1'\psi_3}(t', t), \quad (10)$$

with the matrix element of the reduced density operator of the molecule $P_{\psi_2}^{\psi_1}(t) = \langle\psi_1|\rho_{\text{mol}}(t)|\psi_2\rangle$. Here $|\psi_i\rangle$ are the reduced and oxidized eigenstates of the molecule, i.e., $H_{\text{mol}}|\psi_i\rangle = \varepsilon_{\psi_i}|\psi_i\rangle$, and the irreducible self-energy $\Sigma_{\psi_2'\psi_3}^{I_r\psi_1'\psi_3}(t', t)$ describes possible charge migration processes between the molecule and the leads while interacting with the solvent (see the Supplemental Material [24] for more details). We exploit the Markov approximation by assuming that all solvent relaxation
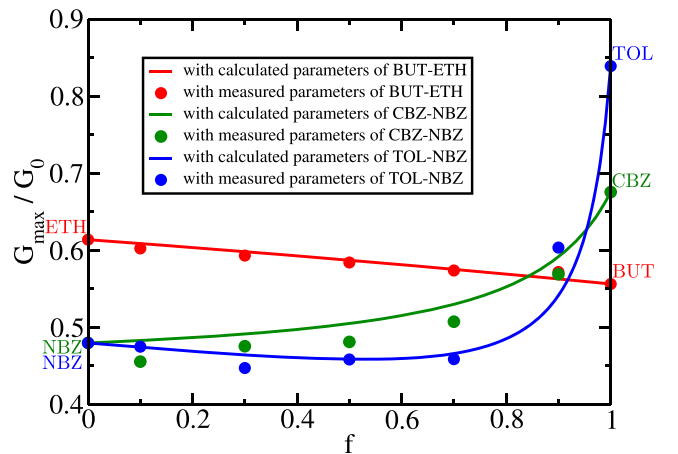


FIG. 3. Maximum of the nonlinear differential conductance as a function of the volume fraction $f$ for the binary mixtures between butanol and ethanol, chlorobenzene and nitrobenzene, as well as toluene and nitrobenzene. The solid lines show the results calculated using the Gladstone-Dale effective dielectric parameters [Eq. (6)] in an effective Debye spectral density. In addition, the circles mark the conductance calculated with a single Debye spectral density of the mixture with the directly measured dielectric parameters taken from Ref. [29]. Parameters are $a = 5$ Å, $\Delta\mu = 5$ D, $T = 0.1\,\Gamma$, $\varepsilon_d = 1.2\,\Gamma$, and $\Gamma = 250$ meV.

processes are fast between two subsequent charge migration processes, so that we neglect memory effects for the electron $\rho_{\text{mol}}(t') \simeq \rho_{\text{mol}}(t)$. Then, in this sequential tunneling regime, the irreducible self-energy turns out to depend only on the time difference $\tau = t - t'$ and consists of four summands of similar form such as

$$\Sigma^{I_r \psi'_1 \psi_3}_{\psi'_2 \psi_3}(\tau) = i\frac{\Gamma}{2\beta} \langle \psi_3 | d^\dagger | \psi'_1 \rangle \langle \psi'_2 | d | \psi_3 \rangle$$

$$\times \frac{e^{i(\varepsilon_{\psi'_1} - \varepsilon_{\psi_3})\tau} e^{-W(\tau)} e^{+i\mu_r(\tau - \frac{i}{B})}}{\sinh\left[\frac{\pi}{\beta}\left(\tau - \frac{i}{B}\right)\right]} + \cdots, \quad (11)$$

where $B$ is the bandwidth of the electronic leads (see the Supplemental Material [24] for more details) and $\beta = T^{-1}$ is the inverse thermal energy. The exponent $W(\tau)$ is found to be [26–28]

$$W(\tau) = \int_0^\infty \frac{d\omega}{\pi} \frac{J(\omega)}{\omega^2} \left[ (1 - \cos(\omega\tau)) \coth\left(\frac{\beta\omega}{2}\right) \right.$$

$$\left. + i \sin(\omega\tau) \right], \quad (12)$$

where $J(\omega)$ is the spectral density of the solvent. The Fourier transform $P^\pm(\omega) = \frac{1}{2\pi} \int d\tau e^{i\omega\tau} e^{W(\pm\tau)}$ describes the probability that an electron absorbs ($P^+$) or emits ($P^-$) the boson energy $\omega$ [26–28]. Finally, we obtain the stationary current $\langle I \rangle_\infty = \langle I_r \rangle_\infty = \lim_{t \to \infty} \langle I_r(t) \rangle$, which is equal in both leads. This result is used to investigate the influence of the solvent on the current-voltage characteristics $I(V)$ as well as on the nonlinear differential conductance $G = dI/dV$. In the following, we set $\Gamma = 250$ meV so that a temperature of $T = 0.1\,\Gamma$ corresponds to room temperature (300 K). The dielectric relaxation parameters of the respective solvents were used from Refs. [29,30]. Additionally, we consider a realistic molecular radius $a = 5$ Å, and a typical dipole moment change of $\Delta\mu = 5$ D [18–22,31].

Figure 1 shows the nonlinear conductance curve of the molecular junction dissolved in the pure solvents toluene (TOL), chlorobenzene (CBZ), ethanol (ETH), butanol (BUT), water (WAT), and nitrobenzene (NBZ). The maximum of the differential conductance is reduced and its width is enhanced when the junction is immersed in a solvent (gray dashed line for the case in absence of a solvent vs solid curves with a solvent in Fig. 1). This is due to the fact that a part of the electric potential energy $eV$, inducing the electric current, is used for the reorganization of the solvent. Therefore, the larger the reorganization energy of the solvent is, the smaller the conductance maximum becomes. Furthermore, the additional tunneling broadening occurs via the absorption or emission of bosonic modes similar to the broadening dominated by the emission of phonons into a substrate [32]. Frank-Condon steps are not present in our case because the dielectric provides a continuum of modes instead of a single mode and since temperature is higher.

To examine the influence of binary solvent mixtures, we have determined the maximum of the differential conductance $G_{\text{max}}$ and have varied the volume fraction $f$. The results are shown in Fig. 3. We find that $G_{\text{max}}$ is highly sensitive to both the volume fraction and the individual solvents themselves. While the conductance for CBZ-NBZ and BUT-ETH
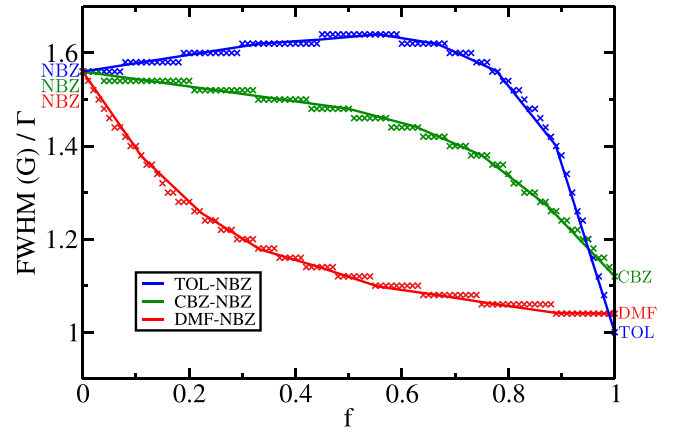


FIG. 4. Full width at half maximum of the nonlinear differential conductance as a function of the volume fraction $f$ for the binary solvent mixtures between nitrobenzene-toluene, nitrobenzene-chlorobenzene, and nitrobenzene-dimethylformamide. The data points have been calculated with an accuracy determined by the voltage step size of $0.02\,\Gamma$, and we have used a cubic spline interpolation for the final curves (solid lines). Parameters are $a = 5$ Å, $\Delta\mu = 5$ D, $T = 0.1\,\Gamma$, $\varepsilon_d = 1.2\,\Gamma$, and $\Gamma = 250$ meV.

monotonously increases or decreases, respectively, the result for TOL-NBZ shows a nonmonotonous behavior. The latter originates in the nonmonotonous dependence of the spectral density of the solvent mixture on the volume fraction; see Fig. 2. Notably, we find an excellent agreement when we compare the dependence of $G_{\text{max}}$ calculated with an effective Gladstone-Dale-Debye solvent mixture of Eq. (6) with the differential conductance calculated with a single Debye solvent with the actual measured dielectric parameters of the binary mixture directly as obtained in Ref. [29] (symbols in Fig. 3). Additional conductance data are shown in the Supplemental Material [24]. Hence, the Gladstone-Dale model of dielectric mixtures can be a sensitive tool to directly read off the volume fraction of binary solvent mixtures.

A measure complementary to the maximum of the differential conductance is the full width at half maximum (FWHM), which we have calculated for the solvent mixtures between toluene-nitrobenzene, chlorobenzene-nitrobenzene, and dimethylformamide-nitrobenzene. The results are shown in Fig. 4. The accuracy of our results is determined by the voltage step size of $0.02\,\Gamma$, and we have used a cubic spline interpolation to show the general trend without extensively exhausting numerical expenses. It can be nicely observed that the FWHM directly follows the behavior of the spectral density or the reorganization energy when comparing with Fig. 2(b).

## V. COMPARISON TO EXPERIMENTAL DATA

Finally, we compare the experimental results of the differential conductance of Ref. [11] with our theoretical results. In the experiment, the electronic conductance of OPE-SMe placed between two gold electrodes and additionally embedded in a solvent has been measured for varying volume fractions of different solvent mixtures. The nonlinear differential conductance of this single-molecule junction can
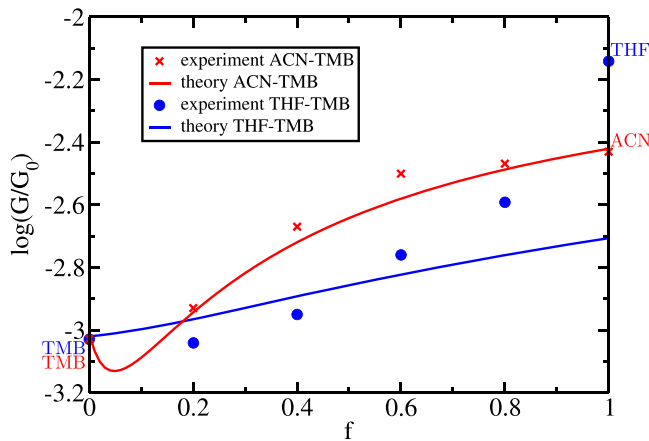
FIG. 5. Nonlinear differential conductance of a OPE-SMe molecular junction as a function of the volume fraction $f$ for binary solvent mixtures of ACN and TMB (red) as well as of THF and TMB (blue). Parameters are $a = 5$ Å, $\Delta\mu = 10$ D, $T = 10\,\Gamma$, $\varepsilon_d = 120\,\Gamma$, and $\Gamma = 2.5$ meV. Experimental data are taken from Ref. [11].

be tuned by nearly an order of magnitude by varying the polarity of the solvent. To recover the experimental data by our model we use the static dielectric constants and the dielectric relaxation times from literature (see Table S1 in the Supplemental Material [24]) for the three investigated solvents 1,3,5-trimethylbenzene (TMB), tetrahydrofuran (THF), and acetonitrile (ACN) and adjust the high-frequency dielectric constants as fitting parameters. In Ref. [11] the length of the molecular junction has been determined by the break-junction technique to be stable around 1 nm. Thus, we choose a radius of $a = 5$ Å. Moreover, we set the dipole moment change to $\Delta\mu = 10$ D, which is in the typical range of OPE-SMe molecular junctions [18–22,31], and $\Gamma = 2.5$ meV so that a temperature of $T = 10\,\Gamma$ corresponds to room temperature (300 K).

Figure 5 depicts the logarithm of the differential conductance calculated at a voltage corresponding to the dot energy of $\varepsilon_d = 120\,\Gamma$ and normalized to the conductance quantum $G_0 = 2e^2/h$ for varying volume fractions between the host solvent TMB and the two inclusions THF and ACN, respectively. A very good agreement between theory and experiment is achieved for the solvent mixture between TMB and ACN (red in Fig. 5). For TMB and THF (blue in Fig. 5), a good alignment between experiment and theory is obtained for volume fractions below 0.8.

In order to explore the mechanism of solvent gating on the charge transport, control experiments with other bridge molecules, which did not exhibit a significant solvent induced shift on the conductance, have been reported in Ref. [11]. In addition, the local density of states (LDOS) has been calculated by means of DFT calculations for all investigated molecules [11]. Only for OPE-SMe, the LDOS was found to be mainly localized on the molecular bridge itself, while for the other molecules, the LDOS was shown to be delocalized almost equally over the gold electrodes as well as the molec-

ular bridge. Hence, only for OPE-SMe does strong LDOS localization on the molecule imply a weak hybridization coupling between the molecule and the electrodes together with a strong influence of the solvent, in agreement with the assumption of sequential tunneling of this work. In addition, the precise form of the investigated molecules as well as the spatial distribution of the LDOS on the molecule do not follow a perfect spherical geometry, which we assume in our model. Hence, deviations between our calculations and the experimental data, such as for the conductance of THF, can occur for these reasons. Moreover, the influence of the solvent on the transmission spectra for OPE-SMe was investigated [11]. The solvent effect on the spectral shift is almost twice as pronounced for ACN as compared to THF, which further supports the very good agreement of our results for ACN. The less pronounced spectral shift for THF in comparison to ACN might be directly related to the polarity of the solvents, which is roughly twice as large for ACN compared to THF [31]. A more polar solvent in turn might lead to a stronger influence on the electron density distribution of the solute and, thus, to a stronger localization on the bridge molecule [33].

## VI. CONCLUSIONS

We provide a theory to calculate the charge current through a molecular junction surrounded by a polar solvent. It describes the influence of pure solvents as well as of binary solvent mixtures on the junction's nonlinear differential conductance. We have used a quantum mechanical real-time diagrammatic technique in the regime of sequential charge tunneling, which includes the electrostatic molecule-solvent coupling in the single electron transfer non-perturbatively. For the solvent mixtures, we use the Gladstone-Dale approach to determine the effective dielectric function and propose an expression for the resulting spectral density of the polarization fluctuations of the solvent mixture. We believe that this approach could be also relevant for optical absorption spectroscopy of solutes in solvent mixtures. Using the measured dielectric constants of pure solvents as well as their respective relaxation times together with tuning the volumetric fraction, we have obtained a very good agreement of the nonlinear differential conductance either calculated by the proposed model and experimentally measured conductance values. Therefore, the proposed theoretical methodology may be applied for a molecular sensor to determine solvent concentrations with high accuracy. Possible extensions of the model could be the inclusion of explicit time-dependent solvent dynamics [34] or solvent viscosity [35].

[1] F. Evers, R. Korytár, S. Tewari, and J. M. van Ruitenbeek, Advances and challenges in single-molecule electron transport, Rev. Mod. Phys. **92**, 035001 (2020).

[2] A. Aviram and M. A. Ratner, Molecular rectifiers, Chem. Phys. Lett. **29**, 277 (1974).

[3] K. S. Kwok and J. C. Ellenbogen, Moletronics: Future electronics, Mater. Today **5**, 28 (2002).

[4] L. Wang, L. Wang, L. Zhang, and D. Xiang, Advance of mechanically controllable break junction for molecular electronics, in *Molecular-Scale Electronics*, edited by X. Guo (Springer, Cham, 2019), pp. 45–86.

[5] H. Park, J. Park, A. K. Lim, E. H. Anderson, A. P. Alivisatos, and P. L. McEuen, Nanomechanical oscillations in a single-$C_{60}$ transistor, Nature (London) **407**, 57 (2000).

[6] Z. Li, M. Smeu, S. Afsari, Y. Xing, M. A. Ratner, and E. Borguet, Single-molecule sensing of environmental pH—An STM break junction and NEGF-DFT approach, Angew. Chem. Int. Ed. **53**, 1098 (2014).

[7] J. K. Sowa, J. A. Mol, and E. M. Gauger, Marcus theory of thermoelectricity in molecular junctions, J. Phys. Chem. C **123**, 4103 (2019).

[8] N. A. Zimbovskaya, Seebeck effect in molecular junctions, J. Phys.: Condens. Matter **28**, 183002 (2016).

[9] Y. Kim, W. Jeong, K. Kim, W. Lee, and P. Reddy, Electrostatic control of thermoelectricity in molecular junctions, Nat. Nanotechnol. **9**, 881 (2014).

[10] M. L. Perrin, E. Burzurí, and H. S. van der Zant, Single-molecule transistors, Chem. Soc. Rev. **44**, 902 (2015).

[11] Z. Tang, S. Hou, Q. Wu, Z. Tan, J. Zheng, R. Li, J. Liu, Y. Yang, H. Sadeghi, J. Shi *et al.*, Solvent-molecule interaction induced gating of charge transport through single-molecule junctions, Sci. Bull. **65**, 944 (2020).

[12] S. Yeganeh, M. Galperin, and M. A. Ratner, Switching in molecular transport junctions: Polarization response, J. Am. Chem. Soc. **129**, 13313 (2007).

[13] J. Zhang, A. M. Kuznetsov, I. G. Medvedev, Q. Chi, T. Albrecht, P. S. Jensen, and J. Ulstrup, Single-molecule electron transfer in electrochemical environments, Chem. Rev. **108**, 2737 (2008).

[14] A. Nitzan, *Chemical Dynamics in Condensed Phases* (Oxford University Press, Oxford, 2006).

[15] V. May and O. Kühn, *Charge and Energy Transfer Dynamics in Molecular Systems* (Wiley-VCH, Weinheim, 2011).

[16] L. Onsager, Electric moments of molecules in liquids, J. Am. Chem. Soc. **58**, 1486 (1936).

[17] J. Gilmore and R. H. McKenzie, Spin boson models for quantum decoherence of electronic excitations of biomolecules and quantum dots in a solvent, J. Phys.: Condens. Matter **17**, 1735 (2005).

[18] L. J. Richter, C. S.-C. Yang, P. T. Wilson, C. A. Hacker, R. D. van Zee, J. J. Stapleton, D. L. Allara, Y. Yao, and J. M. Tour, Optical characterization of oligo(phenylene-ethynylene) self-assembled monolayers on gold, J. Phys. Chem. B **108**, 12547 (2004).

[19] Y. Li, J. Zhao, and G. Yin, Theoretical investigations of oligo(phenylene ethylene) molecular wire: Effects from substituents and external electric field, Comput. Mater. Sci. **39**, 775 (2007).

[20] K. Selvaraju, M. Jothi, and P. Kumaradhas, Exploring the charge density distribution and the electrical characteristics of

[21] H. Lissau, R. Frisenda, S. T. Olsen, M. Jevric, C. R. Parker, A. Kadziola, T. Hansen, H. S. J. van der Zant, M. Brøndsted Nielsen, and K. V. Mikkelsen, Tracking molecular resonance forms of donor–acceptor push–pull molecules by single-molecule conductance experiments, Nat. Commun. **6**, 10233 (2015).

[22] R. Frisenda, S. Tarkuc, E. Galan, M. L. Perrin, R. Eelkema, F. C. Grozema, and H. S. J. van der Zant, Electrical properties and mechanical stability of anchoring groups for single-molecule electronics, Beilstein J. Nanotechnol. **6**, 1558 (2015).

[23] J. H. Gladstone and T. P. Dale, XIV. Researches on the refraction, dispersion, and sensitiveness of liquids, Philos. Trans. R. Soc. London **153**, 317 (1863).

[24] See Supplemental Material at http://link.aps.org/supplemental/10.1103/PhysRevB.106.075413 for detailed expressions of the spectral density parameters for solvent mixtures, a list of dielectric relaxation parameters, a detailed account to calculate the charge current, and more results on the volume-fraction dependence of the nonlinear differential conductance. See also Refs. [36–40].

[25] C.-P. Hsu, Reorganization energies and spectral densities for electron transfer problems in charge transport materials, Phys. Chem. Chem. Phys. **22**, 21630 (2020).

[26] J. König, H. Schoeller, and G. Schön, Zero-Bias Anomalies and Boson-Assisted Tunneling through Quantum Dots, Phys. Rev. Lett. **76**, 1715 (1996).

[27] J. König, J. Schmid, H. Schoeller, and G. Schön, Resonant tunneling through ultrasmall quantum dots: Zero-bias anomalies, magnetic-field dependence, and boson-assisted transport, Phys. Rev. B **54**, 16820 (1996).

[28] H. Schoeller, Transport Theorie für wechselwirkende Quantenpunkte, Habilitation thesis, Karlsruhe Institut für Technologie, Karlsruhe (1997).

[29] J. Lou, T. A. Hatton, and P. E. Laibinis, Effective dielectric properties of solvent mixtures at microwave frequencies, J. Phys. Chem. A **101**, 5262 (1997).

[30] U. Kaatze, Complex permittivity of water as a function of frequency and temperature, J. Chem. Eng. Data **34**, 371 (1989).

[31] C. Reichardt and T. Welton, *Solvents and Solvent Effects in Organic Chemistry* (John Wiley & Sons, Weinheim, 2011).

[32] S. Braig and K. Flensberg, Vibrational sidebands and dissipative tunneling in molecular transistors, Phys. Rev. B **68**, 205324 (2003).

[33] A. Rondi, Y. Rodriguez, T. Feurer, and A. Cannizzo, Solvation-driven charge transfer and localization in metal complexes, Acc. Chem. Res. **48**, 1432 (2015).

[34] H. Kirchberg, P. Nalbach, and M. Thorwart, Nonequilibrium quantum solvation with a time-dependent Onsager cavity, J. Chem. Phys. **148**, 164301 (2018).

[35] M. F. Gelin and D. S. Kosov, A model for dynamical solvent control of molecular junction electronic properties, J. Chem. Phys. **154**, 044107 (2021).

[36] J. Crossley and S. Walker, Dielectric studies. Part XVIII. Dipole moments and relaxation times of some symmetrically substituted alkylbenzenes, Can. J. Chem. **46**, 847 (1968).

[37] S. Vaish and N. Mehrotra, Correlation of NMR spin lattice and dielectric relaxation times of some methyl benzenes, Indian J. Pure Appl. Math. **37**, 881 (1999).

[38] A. Chaudhari, P. Khirade, R. Singh, S. Helambe, N. Narain, and S. Mehrotra, Temperature dependent dielectric relaxation study of tetrahydrofuran in methanol and ethanol at microwave frequency using time domain technique, J. Mol. Liq. **82**, 245 (1999).

[39] J. Barthel, M. Kleebauer, and R. Buchner, Dielectric relaxation of electrolyte solutions in acetonitrile, J. Solution Chem. **24**, 1 (1995).

[40] G. D. Mahan, *Many-Particle Physics* (Springer Science & Business Media, New York, 2013).